

# Adsorption Properties of Thiol-Functionalized Silica Nanoparticles Prepared for Application in Poly(ether sulfone) Nanocomposite Membranes

Ahmad Rezvani-Boroujeni, Mehran Javanbakht, Mohammad Karimi, and Behrouz Akbari-Adergani

**Abstract**— Thiolfunctionalized silica nanoparticles ( $\text{SiO}_2\text{-SH}$ ) were prepared by sol-gel method through using 3-mercaptopropyltrimethoxysilane and nanosized silica. The effect of the pH of the silane solution on grafting efficiency of silica nano-particles was scrutinized. It was found that the reaction between silane and silica nanoparticles was more effective at low pH. The FTIR spectroscopy and CHNS analyses were used to study the chemistry of the modified nanoparticles. It was found that the  $\text{SiO}_2\text{-SH}$  groups could effectively remove the heavy metal ions ( $\text{Pb}^{2+}$ ,  $\text{Ni}^{2+}$ , and  $\text{Hg}^{2+}$ ) in the solution through electrostatic and chemical interactions. The adsorption isotherm and adsorption capacity of the functional nanoparticles for different metal ions, and its selectivity were investigated. Similarly, the effect of the pH values on the adsorption of metal ions was studied. The strong adsorption ability of  $\text{SiO}_2\text{-SH}$  can be attributed to the functional nanoparticles with rich thiol groups facilitating the mass transport of metal ions to the active sites. These functional nanoparticles were blended in poly(ether sulfone) membranes as an adsorbent to improve the membranes separation and selectivity properties for removal of heavy metal ions.

**Keywords:** adsorption, functionalization, heavy metal, mercapto silane, poly(ether sulfone) membrane, silica nanoparticle

## List of symbols and acronyms

AAS	atomic adsorption spectroscopy
BET	Brunauer–Emmett–Teller
CA	contact angle (deg)
$C_0$	initial concentration of heavy metal ions ( $\text{mg L}^{-1}$ )
FTIR	Fourier-transform infrared spectroscopy
ICP	inductively coupled plasma mass spectroscopy
$K_1$	constant of pseudo-first-order kinetic model
$K_2$	constant of pseudo-second-order kinetic model
$K_L$	Langmuir constant
$K_F$	Freundlich capacity factor
$M$	weight of silane (g)
$m$	weight of nanoparticle (g)

$m_{\text{Si}}$	weight of silica (g)
$M_{\text{Silane}}$	molecular weight of silane
TFNS	thiol functionalized nanosilica
MPTMS	3-mercaptopropyltrimethoxy silane
$N_A$	Avogadro constant
$N_{\text{OH}}$	number of hydroxyl groups per $\text{nm}^2$ on silica surface
$1/n$	Freundlich intensity parameter
PES	poly(ether sulfone)
$q_e$	adsorption capacity ( $\text{mg g}^{-1}$ )
$q_{e\text{np}}$	adsorption capacity of nanoparticles in the membrane ( $\text{mg g}^{-1}$ )
$q_{e\text{m}}$	adsorption capacity of membrane ( $\text{mg m}^{-2}$ )
$S_{\text{Si}}$	surface area of silica nanoparticle ( $\text{nm}^2$ )
SEM	scanning electron microscopy
TGA	thermal gravimetric analysis
$V$	solution volume (L)

## I. INTRODUCTION

Recently, the presence of heavy metals in the polluted waters has become an area of widespread environmental concern presenting significant hazards to the human health. Hg, Pb, Cd, and Ni are considered as the most hazardous metals and are on the US Environmental Protection Agency's list of priority pollutants. Various separation techniques have been used for treatment of wastewater containing heavy metal ions, including ion exchange [1], solvent extraction [2], adsorption [3], precipitation [4], and membrane separation [5,6]. These conventional methods are generally useful, but when they are applied to dilute solutions, they are costly, and more importantly, they show little/no selectivity.

Metal adsorption onto the solid phase, which is simple, inexpensive, and efficient, has been proposed as a suitable method for mercury extraction. Natural and synthetic adsorbents, including activated carbon, chelate resins, chitosan, zeolite and fly ash have been considered [7-11]. Whereas the selectivity of common complexing ligands (such as activated carbon and soluble polymers) due to their physically adsorption as a result of van der Waals forces, are not efficient. Therefore, looking for a novel adsorbent with high selectivity via chemical interaction is interested. In the recent years, many researchers have focused on the use of functional nanoparticles.

Some researchers believe that the surface area and pore size of silica based materials affect their absorbability for heavy metals [3,12]. A higher surface area and a bigger pore size will lead to more active sites for the adsorption of

A. R. Boroujeni and M. Javanbakht are with the Department of Chemistry, Amirkabir University of Technology, Tehran, Iran. M. Karimi is with the Department of Textile Engineering, Amirkabir University of Technology, Tehran, Iran. B. A. Adergani is with the Food and Drug Laboratory Research Center, Food and Drug Organization, Ministry of Health and Medical Education, Tehran, Iran. Correspondence should be addressed to M. Javanbakht (e-mail: [javanbakht@aut.ac.ir](mailto:javanbakht@aut.ac.ir)).

heavy metals [13]. Interestingly, scrutiny of the experimental results of the literature indicate that the type of the functional groups grafted onto the support plays an important role in determining the adsorption capacity for heavy metals, regardless of the type and structure of the adsorbent [14,15]. For example, the maximum adsorption capacity of thiol functionalized MCM-41 adsorbents, with a surface area of  $422 \text{ m}^2 \text{ g}^{-1}$ , for adsorption of  $\text{Pb}^{2+}$  was  $66 \text{ mg g}^{-1}$  [16], while the adsorption capacity of thiol-functionalized mesoporous silica with a surface area of  $321 \text{ m}^2 \text{ g}^{-1}$  was  $91.5 \text{ mg g}^{-1}$  [17].

Consequently, the high surface area and pore size are not the main factors in determining the adsorption capacity; i.e. they cannot guaranty a high adsorption capacity. Although, the higher surface area of the particles has the potential for providing more active sites for surface functionalization [13,15]. The number of functional groups on the adsorbent surface is a more important factor than surface area and pore volume in determining the adsorption capacity [16], since the adsorption of adsorbates is achieved through interacting with the functional groups on the adsorbents surface by means of either chemical bonding or physical adsorption [15,18].

The effectiveness of adsorbents to bind with metal ions has been attributed to the complex formation between ligands and metal ions. The specificity of a particular ligand toward target metal ions is the result of a conventional acid–base interaction between them [19]. Therefore, as an ideal adsorbent, the surface area should be as large as possible and the surface chemistry modification should be easy. The high surface area of nanoparticles provide suitable situation for the heavy metal uptake; and the functional groups of nanoparticles play an important role in its selectivity due to the affinity between the functional groups and the solute molecules [20].

Surface functionalization is a useful method by which the loading capacity and selectivity of an adsorbent can be significantly enhanced. In the past years, we described the use of functionalized nanoporous silica gels with different grafting moiety such as 1,3-dicyclohexyl-2-propylguanidine [21], phenylthiourea [22], and dipyrindyl [23,24] for selective determination or separation of various heavy metal ions in aqueous solutions. We showed that thiourea-functionalized nanoporous silica can be used as a selective material to monitor  $\text{Hg(II)}$  ions in waste water and fish samples [25]. Some research works demonstrate that the functional groups determine the selectivity of an adsorbent. Adsorbents with sulfur functionality, like thiol groups, show high affinity for  $\text{Hg}^{2+}$  and  $\text{Pb}^{2+}$  ions [26-28].

The use of various silane coupling agents with several functionalities is a typical method for functionalization of inorganic nanoparticles which are employed to separate heavy metal ions from aqueous solutions. Sol-gel method, shown schematically in Fig. 1, introduces a simple and useful method which is generally employed for this purpose. Organosilane functional nanoparticles are becoming very useful materials for the separation of toxic heavy metal ions from aqueous solutions because of the rapid adsorption, high affinity, various functionality, and

selectivity towards different metal ions for selective separation. Recently, thiol- functional silane coupling agents, like mercaptopropyl trimethoxysilane, have been used to prepare effective adsorbents for various heavy metal ions [14-17].

Polyethersulfone (PES) is one of the most important polymeric materials widely used in separation fields due to its good mechanical and chemical properties, and easy preparation by the phase inversion method [29]. PES and PES-based membranes have some disadvantages, too. The main disadvantage of PES membranes is their hydrophobic characteristic and non-selective separation. Recently, the use of nanoparticles in modification of polymeric membranes, as a very simple and useful technique, has been studied by researchers [30]. These inorganic nanoparticles can be entrapped in membrane matrix and form a nanocomposite membrane [31], or deposit on the membrane surface [32]. Hydrophilic nanoparticles can improve the membrane hydrophilicity [30,33]. Previously, the main aim of using inorganic nanoparticles in membranes was to increase the hydrophilicity and decrease the fouling problem [30,33], whereas less attention was paid to the improvement of the membrane selectivity for special target materials such as heavy metal ions. Consequently, use of a suitable functional nanoparticle can improve the membrane properties even more by acting as an adsorbent agent and improving the membrane selectivity and separation properties.

In our previous work, prepared thiol-functionalized silica nanoparticles were immobilized on PES membranes and the separation properties of these modified membranes for Hg ions was investigated in a filtration process [6]. In this work, some adsorption properties (such as adsorption kinetic and isotherm) of thiol-functionalized nanosilica (TFNS) for Hg, Pb and Ni ions were scrutinized. The TFNS particles were prepared via sol gel reaction between silica nanoparticles and 3-mercaptopropyletrimethoxy silane. The effect of the pH of the silane solution on grafting efficiency of silica Nano-particles was investigated. The FTIR spectroscopy, CHNS analysis and thermal gravimetric analysis (TGA) were employed to investigate the efficacy of surface functionalization on silica particles. Adsorption properties of TFNS particles for Hg, Pb and Ni ions were studied with a batch technique. Adsorption kinetics and isotherms of TFNS were investigated to predict the adsorption behavior of modified nanoparticles. Finally, these functional nanoparticles as a good adsorbent were blended in poly(ether sulfone) membrane matrix and the adsorption properties of these nanocomposites were investigated.

## II. EXPERIMENTAL

### A. Materials

Gama-mercaptopropyltrimethoxysilane (MPTMS) (A-189) provided from Wacker Company and silica nanoparticles (Arosil 200) - see Table I for specifications-supplied from Degussa Company were used for the preparation of thiol functional nanosilica. Other raw materials such as  $\text{HgCl}_2$  (99.6%),  $\text{NiCl}_2$  (99.7%),  $\text{Pb}(\text{NO}_3)_2$

(99.3%), HCl, H<sub>2</sub>SO<sub>4</sub>, EtOH (99.9%), and HNO<sub>3</sub> were purchased from Merck.

TABLE I  
PROPERTIES OF SILICA NANOPARTICLES

SiO <sub>2</sub> content	>99.8
OH content	4.6 OH nm <sup>-2</sup>
pH of 4 wt% dispersion	3.7 – 4.7
average particle size	12 nm
specific surface area (BET)	200 m <sup>2</sup> g <sup>-1</sup>
bulk density (g L <sup>-1</sup> )	~ 30

### B. Preparation of Functional Nanoparticle

The surface functionalized nanosilica particles were prepared with 3-mercaptopropyltrimethoxy silane coupling agent by applying the well-known sol-gel method. The Functionalization mechanism is schematically shown in Fig. 1. Silica nanoparticles were refluxed in a glass round bottom flask equipped with a Graham condenser and a heating oil bath. The amount of silane was calculated according to a stoichiometric value related to the amount of silica and hydrolysis ratio of 3 as follows [34,35]:

$$M = \frac{3 \times S_{Si} \times m_{Si} \times M_{Silane} \times N_{OH} \times 10^{19}}{NA} \quad (1)$$

where  $M$ ,  $S_{Si}$ ,  $m_{Si}$ , and  $M_{Silane}$  are the amount of added silane (g), the surface area of silica, the weight of silica, and the molecular weight of silane, respectively.  $N_{OH}$  is the number of hydroxyl groups per nm<sup>2</sup> on silica surface; and the hydrolysis ratio (the ratio of water to silane) is 3. A mechanical homogenizer (IKA) was used for the samples at 13,000 rpm. Silica nanoparticles were stirred for 30 min at an adjusted pH (in the range of 1 to 6, adjusted by adding one molar HCl and NaOH solutions). Then MPTMS was poured drop-wise at the rate of 0.5 g min<sup>-1</sup>, and the reaction remained at this condition for 1.5 h (hydrolyzation step). Then the pH was increased to 9 by adding NaOH and remained for 1 h (condensation step) before centrifuging the mixture at 5,000 rpm [35]. The thiol-functional nanosilica samples prepared at pH 1, 4 and 6 were coded as TFNS-1, TFNS-2 and TFNS-3 respectively.

The samples were washed 3 times with ethanol and in each washing stage, the suspensions were centrifuged. Then the sediment particles were dispersed in water:ethanol (50:50) and were dried by using a spray dryer at 110 °C [35].

### C. Membrane Preparation

Flat sheet PES membranes were prepared by phase inversion technique. A homogenous polymeric casting solution containing 18 wt% PES, 1 wt% PVP as pore former, and DMAC as solvent was prepared. After achieving a homogenous solution, it was casted using an adjustable casting knife (150 μm) on a glass plate and then immediately immersed into de-ionized water (DIW) coagulation bath at 25 °C. All films remained in DIW for one week and then dried for a day at 25 °C. Nanocomposite

membranes were prepared by the same procedure and adding 1 and 2 wt% TFNS into the casting solution.

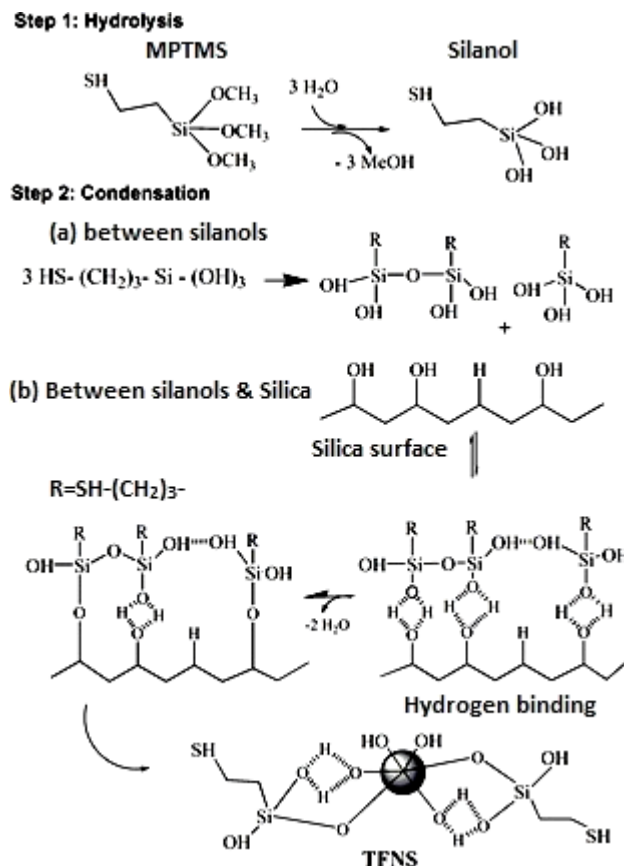


Fig. 1. Functionalization mechanism of nanosilica with MPTMS through sol gel reaction.

### D. Characterization

Fourier Transform Infrared spectroscopy (FTIR) and CHNS elemental analysis were used for the chemical analysis of functional silica nanoparticles. FTIR technique using Bruker-IFS 48 FTIR spectrometer (Etlingen, Germany) with horizontal ATR device (Ge, 45°) was used. 32 scans were taken with a 4 cm<sup>-1</sup> resolution in the range of 4000 to 500 cm<sup>-1</sup>. To investigate the efficacy of surface treatment, the thermal gravimetric analysis (TGA) and CHNS elemental analysis were performed. CHNS elemental analysis was carried out by ASTM-D5291 method. TGA analysis was done by TA, Q50 instrument on about 1.5 g of the sample in an aluminum cup, at a heating rate of 10 °C min<sup>-1</sup> (from ambient temperature up to 600 °C) under nitrogen atmosphere.

For morphological investigation, E-SEM (Philips-X130, Netherland) was employed. The nanoparticles dispersed in acetone with ultrasonic probe, and then the dispersion was sprayed on a glass sheet. These dried samples were gold sputtered for producing electric conductivity, and electron-micrographs were taken under very high vacuum conditions at 15 kV.

Inductively coupled plasma mass spectroscopy (ICP) and atomic adsorption spectroscopy (AAS) were used for the detection of sorption performance of functional silica nanoparticles and PES nanocomposites. The surface hydrophilic/hydrophobic properties were evaluated based

on the water contact angle (CA) and the amount of water vapor adsorbed on to the surface of the modified particles. The water contact angles (CA) of the silica samples were measured using a contact angle analyzer (Phoenix 300, SEO). The contact angle of water was measured on the membranes surface using tensiometer, G10 KRUSS, Germany. DIW was used as the probe liquid in all measurements. To minimize the experimental error, the contact angles were measured at five random points of each sample and the average number was reported.

The membrane porosity ( $\varepsilon$ %) defined as the volume of the pores divided by the total volume of the porous membrane was determined by the gravimetric method using Eq. (2) and measuring the weight of the pure water that had filled the membrane pores [31].

$$\varepsilon = \frac{(w_{wm} - w_{dm}) / \rho_w}{(w_{wm} - w_{dm}) / \rho_w + w_{dm} / \rho_p} \quad (2)$$

where  $\varepsilon$  is the membrane porosity,  $w_{wm}$ ,  $w_{dm}$ ,  $\rho_w$ , and  $\rho_p$  are the weights of wet membrane (g), the weight of dry membrane (g), the pure water density ( $0.998 \text{ g cm}^{-3}$ ), and the polymer density, respectively. Since the inorganic content of the membrane matrix was small,  $\rho_p$  was approximately equal to the density of PES, namely  $1.37 \text{ g cm}^{-3}$ .

#### E. Adsorption Property

The ability of the modified silica nanoparticles with thiol functional groups (-SH) to remove Pb(II), Ni(II) and Hg(II) ions from aqueous solutions was investigated by a batch technique. The adsorption efficiency of TFNS was carried out in 20 mL flasks containing 3 to 40 ppm of  $\text{Hg}^{+2}$ ,  $\text{Pb}^{+2}$  and  $\text{Ni}^{+2}$  solution prepared with  $\text{HgCl}_2$ ,  $\text{Pb}(\text{NO}_3)_2$ , and  $\text{NiCl}_2$ . One mg of TFNS as adsorbents was added to each flask. The flasks were sonicated for 30 min to disperse the nanoparticles and form homogenous suspensions. Then, the suspensions were shaken at  $25^\circ\text{C}$  and 500 rpm in a thermostatic shaker. 0.1 mol HCl and 0.1 mol NaOH solutions were used for the pH adjustment. Finally, the suspensions were centrifuged at a speed of  $6000 \text{ rpm min}^{-1}$  and filtered. The concentration of metal ions in aqueous samples was measured by ICP technique. The amount of metal ions adsorbed per unit mass of the adsorbents ( $q_e$ ) was calculated by the following equation:

$$q_e = \frac{(C_0 - C_e) \times V}{m} \quad (3)$$

where  $C_0$  and  $C_e$  are the initial and final concentration of ions, respectively,  $V$  is the solution volume, and  $m$  is the mass of the nanoparticles, respectively.

The adsorption capacity of TFNS in nanocomposite membranes ( $q_{e,np}$ ), is defined as the amount of Hg ions adsorbed per unit mass of TFNS in the nanocomposite, was calculated by Eq. (4). For this purpose, the amounts of adsorbed Hg ions were divided by the amount of nanoparticles in the membrane. Adsorption capacity of membranes ( $q_{e,m}$ ) was calculated as milligram of Hg ions per unit area of the membrane, as described previously [6].

The amount of Hg ions that were adsorbed per unit mass of the membranes was calculated by Eq. (5).

$$q_{e,np} = \frac{(C_0 - C_e) \times V}{M_{np}} \quad (4)$$

$$q_{e,m} = \frac{(C_0 - C_e) \times V}{A_m} \quad (5)$$

where  $C_0$  and  $C_e$  are the initial and final concentration of Hg ions in solution, respectively,  $V$  is the solution volume,  $M_{np}$  is the weight of TFNS in each membrane and  $A_m$  is the effective membrane area.

### III. RESULTS AND DISCUSSION

#### A. Chemical Analysis

The chemical structure of silica and TFNS analyzed by FTIR is shown in Fig. 2 and the main FTIR peaks are described in Table II.

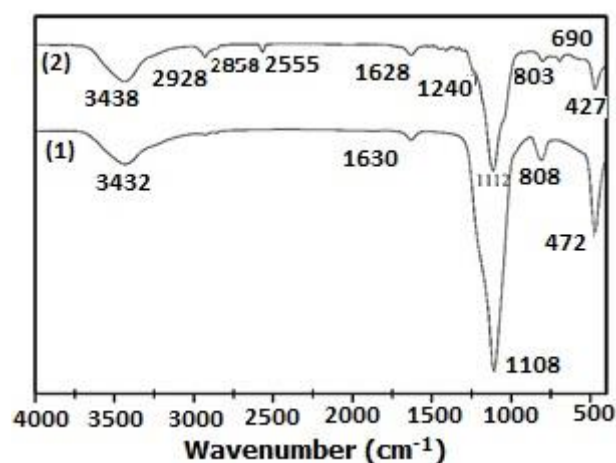


Fig. 2. FTIR graph of (1) silica, and (2) functionalized silica nanoparticles.

TABLE II  
MAIN FTIR PEAKS OF TFNS PREPARED BY THE SOL-GEL METHOD

groups	peak ( $\text{cm}^{-1}$ )
Si-O-Si	472 808 1108
S-H	2555
CH	2928-2658
OH	1635
silanol	3433

A sharp Si-O-Si stretching peak ( $1010\text{--}1190 \text{ cm}^{-1}$ ) is observed for both modified and unmodified samples. The peak at  $800\text{--}900 \text{ cm}^{-1}$  corresponding to the -Si-O (silanol) groups can be observed for both samples, confirming that during the functionalization of silica nanoparticles, not all the silanol groups of the surface are consumed. The peak at  $690 \text{ cm}^{-1}$  and the weak peaks around  $1200 \text{ cm}^{-1}$  corresponding to Si-C groups can be observed in the graph (2) of Fig. 2. Due to the presence of this Si-C peak, the Si-O-Si peak in  $1112 \text{ cm}^{-1}$  is wider than that of the pure

silica [35]. The peak observed at 1600–1630  $\text{cm}^{-1}$ , corresponding to  $-\text{OH}$  groups, may be related to the presence of physically adsorbed water. The weak peak observed at 2550  $\text{cm}^{-1}$  is related to  $-\text{SH}$  group and a double peak observed at 2928–2858  $\text{cm}^{-1}$  is due to  $-\text{CH}_2$  stretching bond, which demonstrate that MPTMS is considerably grafted on the nanosilica surface [15,28,35].

The TGA graphs of TFNS-1 and silica nanoparticles are shown in Fig. 3 and the results of CHNS and TGA analysis are shown in Table III.

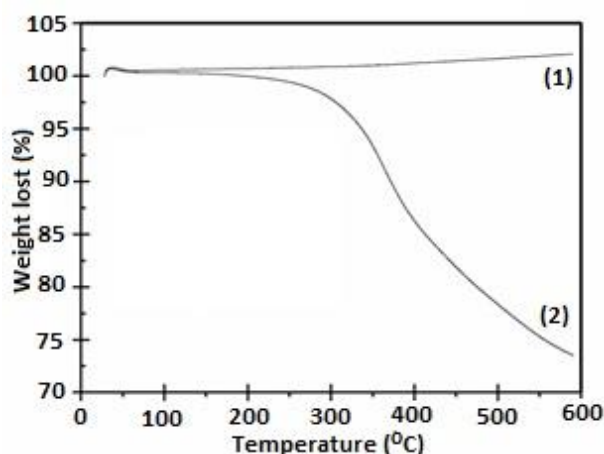


Fig. 3. TGA analysis of (1) unmodified silica nanoparticles, and (2) TFNS.

The weight loss at low temperatures ( $<200\text{ }^\circ\text{C}$ ) could be attributed to the release of adsorbed water and volatiles such as alcohol, while the weight loss in the temperature range of 200–600  $^\circ\text{C}$  is resulted from the decomposition of the grafted MPTMS molecules and the silanol condensate groups. The decomposition of mercaptopropyl groups occurs slowly at 200–400  $^\circ\text{C}$ , followed by a rapid degradation above 400  $^\circ\text{C}$  [35].

TGA results show the weight loss of the modified nanosilica. This weight loss is related to decomposition of functional groups of MPTMS which are grafted on nanosilica ( $-(\text{CH}_2)_3-\text{SH}$ ). These results are similar to the outcomes of elemental analysis for sulfur, carbon and oxygen content in CHNS analysis. By dividing the moles of the functional groups of TFNS that were calculated from TGA or CHNS analysis, by the mole of silica nanoparticles added to the reaction suspension, the grafting fraction of modified nanoparticles ( $\text{mole}_{\text{silane}}/\text{mole}_{\text{silica}}$ ) was obtained. Grafting efficiency is defined as the ratio of the grafting fraction (GF) to the molar ratio of silane/silica in the reaction solution [34,35]. The grafting efficiency is

calculated by using TGA and elemental analysis results. The both calculation methods have good coordination and recognize each other. TFNS-1, which is prepared in pH 1, had more functional groups. According to the chemical structure of the functional group  $-(\text{CH}_2)_3-\text{SH}$ , theoretically, for each mole of sulfur, there are 3 moles of carbon and 7 moles of hydrogen. The elemental analysis of functional silica showed good consistency with the theory, although a little nonconformity for TFNS-1 was observed.

In sol-gel process of silane precursors, hydrolysis and condensation are two simultaneous processes. Fig. 1 shows the reaction steps involved in the silane solution (for 3-mercaptopropyletrimethoxy silane, R is  $-(\text{CH}_2)_3-\text{SH}$ ). In the acidic condition, the hydrolysis is faster than the condensation which causes the number of siloxane groups to increase [35-36]. Under mild acidic condition, neutral alkoxy silane is hydrolyzed rapidly form monomeric silantriol, and then is condensed slowly to form polymeric or organic siloxanol. Hence, in the pH 1, the rate of hydrolysis reaction of silane precursors in the solution (step1 in Fig1) increases, resulting in the formation of more silanol groups in the solution. TGA and Elemental analysis (CHNS analysis) show that the sulfur content of samples prepared at pH 1 were more than that of the samples prepared at pH 6, which is consistent with the described reaction principles. On the other hand, acidic environment creates a suitable situation for formation of high silanol groups in the reaction condition and prevents the co-condensation reaction between them. Besides, gradual addition of silane into the reaction reinforces this prevention. Likewise, the surface protonation of silica nanoparticles increases the adsorption rate of silanol on the silica surface, which helps this hindrance. Therefore, the silanol groups formed in the solution are quickly and immediately adsorbed on the silica surface. Accordingly, in our further investigations TFNS-1 was used as an absorbing agent, which is defined as TFNS in the continuation of the text.

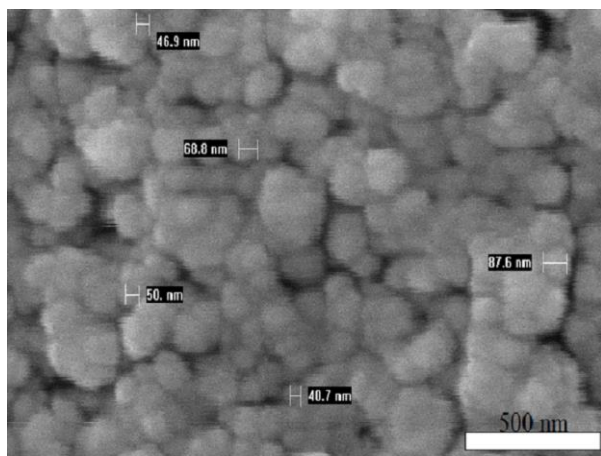
### B. Morphological Study

The SEM images of TFNS are shown in Fig. 4(a), which exhibit that the particle size of the nanoparticles increase after surface modification (reaches from 50 to 70 nm) possibly because of the formation of a silane layer on the surface of nanosilica and/or due to the coupling of nanoparticles along with the silanation process. It can be observed that the shape of the treated sample with the highest amount of grafting is almost similar to that of the unmodified silica. It can be concluded that the morphology

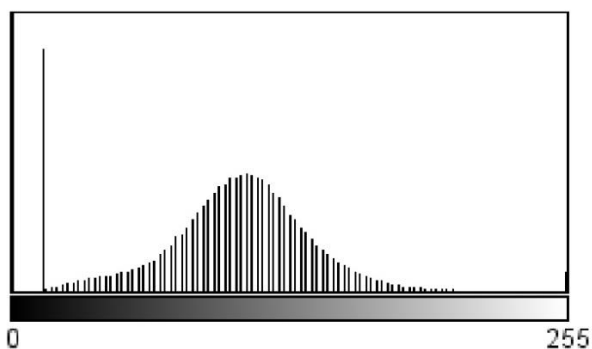
TABLE III  
CHNS AND TGA RESULTS OF MODIFIED AND UNMODIFIED SILICA NANOPARTICLES

PH	CHNS analysis				TGA				
	S	C	H	GF $\text{mmol mol}^{-1}$	grafting efficiency %	weight loss	GF $\text{mmol mol}^{-1}$	grafting efficiency %	
TFNS-1	1	12.83	15.6	3.10	444.74	48.45	28.3	369.77	40.28
TFNS-2	4	10.32	11.6	2.39	291.84	31.79	24.4	293.12	31.93
TFNS-3	6	7.08	7.96	1.61	172.61	18.80	16.3	167.74	18.27

of samples do not considerably change upon grafting. However, the chemistry of particles altered significantly. The histogram of particle size distribution plotted from the SEM image is shown in Fig 4(b).



(a)



Count: 344608      Min: 0  
 Mean: 92.662      Max: 255  
 StdDev: 47.148      Mode: 0 (25461)

(b)

Fig. 4. (a) SEM images of thiol-functionalized silica nanoparticles (TFNS), (b) the histogram of particle size distribution; plotted from the SEM image.

### C. Hydrophilicity

To evaluate the surface hydrophilic/hydrophobic properties of nanoparticles the test samples were prepared by grinding the nanoparticles using a mortar, and pressing the ground powder. The surface wettability of the silica particles was determined by measuring the amount of water adsorbed on the silica surface. Adsorption of water vapor on to the silica surface was performed using a humidifier and a chamber [36]. The particles were put in the chamber and a stream of air and water vapor was flowed into the chamber at 70 °C for 24 h. Before the experiment, the particles were dried in a vacuum oven at 110 °C for 2 h. The wettability values were determined by calculating the weight gain of the silica particles per weight of the particles. This value for the nanosilica and TFNS was 0.51 and 0.11 g(H<sub>2</sub>O)/g(nanoparticle), respectively (Table IV). In an ambient air atmosphere, the molecular water adsorbed on the surface of materials can change the wettability [37].

The introduction of hydrophobic carbon-based chains on TFNS leads to a decrease in the portion of silanol groups on the nanosilica surface, which lowers the hydrophilicity and wettability of the surface. Although hydrophobic propyl chains were introduced on the surface, the surface maintained partially hydrophilic due to the presence of mercapto groups at the end of the chains.

TABLE IV  
 HYDROPHILICITY OF MODIFIED AND UNMODIFIED NANOSILICA

	water contact angle CA	wettability (g <sub>H<sub>2</sub>O</sub> /g )
nanosilica	17.3°	0.51
TFNS	68.8°	0.11

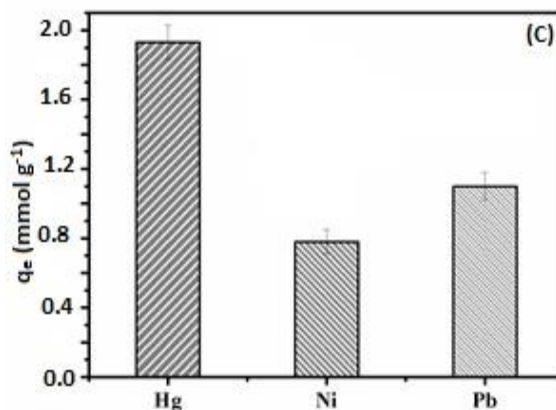
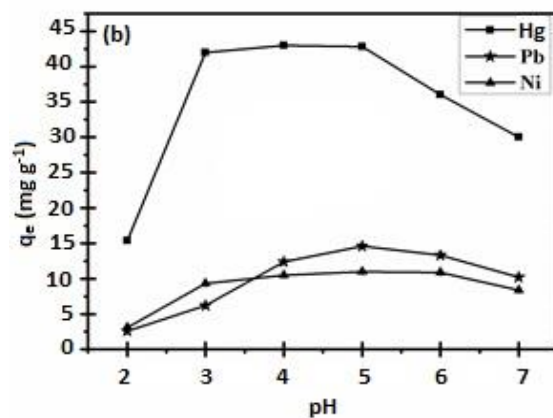
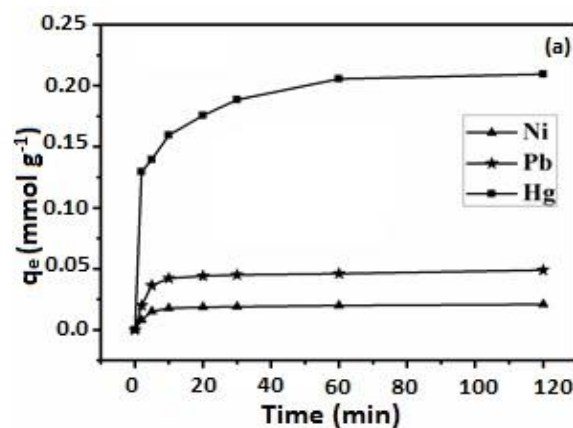


Fig. 5. Adsorption properties of thiol-functionalized nanosilica: (a) adsorption capacity of TFNS for Hg, Pb and Ni ions, (b) Effect of pH on adsorption capacity of TFNS, and (c) adsorption capacity of TFNS for heavy metal ions in the solutions which contain the same concentration of Hg, Ni and Pb ions.

#### D. Adsorption Property

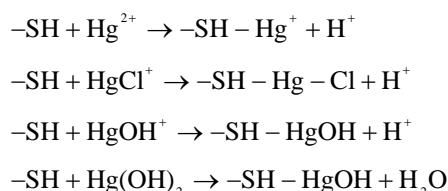
The ability of modified silica nanoparticles with thiol functional groups (-SH), to remove Pb(II), Ni(II) and Hg(II) ions from aqueous solutions was investigated and its results are shown in Fig. 5(a). For heavy metal ions the equilibrium was reached within 2 h and the state of 90% equilibrium was reached in the first 20 min, which indicates the adsorption of heavy metal ions on TFNS. The rate of mass diffusion is quick because all the active adsorption sites are located directly on the surface of the particles. Therefore, very high adsorption capacity was obtained.

Sorption is defined as the transferring of ions from the solution phase to the solid phase via various mechanisms such as physical and chemical adsorption, surface precipitation, or solid-state diffusion or fixation [28]. Adsorption reactions are normally considered as intermolecular interactions among solute and solid phases, which may be described as surface complex adsorption. These complex interactions comprise two reactions between the metal ions and surface functional groups: chemical binding and electrostatic binding. The former leads to specific adsorption (a more selective adsorption), and the latter which is accompanied by formation of complexes leads to non-specific adsorption [15].

Adsorption capacity of TFNS nanoparticles for different heavy metal ions; Pb(II), Ni(II) and Hg(II) in a mixture containing equal concentration of each ion was measured in the same batch technique; Fig. 5(c). Adsorption results indicated that TFNS was more selective for Hg ions than for other ions. The interaction between -SH groups and heavy metal ions is a typical Lewis acid and base interaction which forms covalent bands. According to Pearson theory for hard and soft acids and bases [38], the mercaptan group, due to higher affinity for soft metal ions and its ability to form chemical bonding with them, has high and selective adsorption ability for Hg<sup>2+</sup> as a soft acid. Therefore, in the mixture solution, adsorption capacity of TFNS for Hg<sup>2+</sup>, as a softer metal ion, was considerably more than for Pb<sup>+2</sup> and Ni<sup>+2</sup> ions which are harder metal ions; Fig. 5(c).

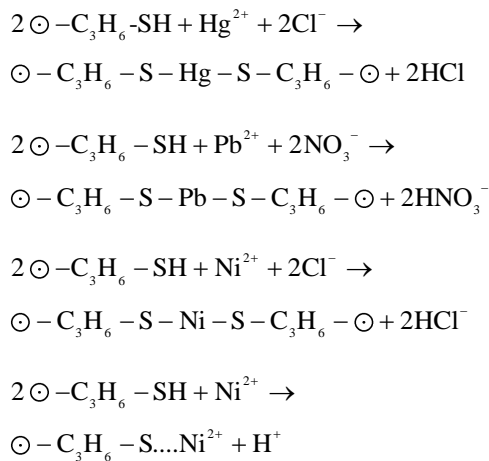
The effect of the pH of the solution on adsorption properties of MPTMS-silica is exhibited in Fig. 5(b). It can be seen that at first, the amount of sorption increases with the increase in pH. This may be because of the protonation of the sulfur atom of the -SH group of TFNS, which diminishes its ability to form chelates with Hg<sup>+2</sup>, Pb<sup>2+</sup> and Ni<sup>2+</sup> ions in aqueous solution at low pH. This indicates the competitive effect of H<sup>+</sup> disruption in the formation of Hg-S, Pb-S and Ni-S bonds [39]. That consequently has an influence on the low removal of metal ions at low pH values. The most efficient removal of Pb(II) and Ni(II) was achieved at a pH range of 4 to 5. The results demonstrated that the adsorption capacity of Hg(II) increased with the increase in the initial pH, and reached a plateau value with a pH in the range of 3.0 to 5.0; Fig. 5(b). Adsorption capacity may be affected both by the species of Hg(II) and the accessibility to the binding sites. The surface charge of TFNS will be considerably affected by switching from

negative to positive when the pH of the solution is altered from basic to acidic [15]. At pH < 3, Hg(II) ion adsorption decreased rapidly where HgCl<sub>2</sub> dominates in the solution; Fig. 5(b). Hg(II) has strong affinity for sulfur donating ligands and halogens [40]. At pH < 3, the decreasing trend in the adsorption of Hg(II) is due to the competition between the formation of mercury-sulfur bonds during the adsorption process onto TFNS particles and the stabilization of the Chloro-complexes (HgCl<sub>2</sub><sup>-</sup>) in the solution [41]. At pH > 7 where Hg(OH)<sub>2</sub> prevails, non-soluble metal hydroxyl may precipitate. The difference in performance over the studied pH range can be related to the stability of the chelate compound attached to the silica material [14], as for TFNS the -S-Hg- bond has a high stability constant [42]. Indeed, the stability of -S-Hg- bond is higher than that of other divalent metal ions with SH groups [43]. As reported [45], depending on the pH of the solutions, in the presence of Cl<sup>-</sup>, different Hg(II) species, i.e., Hg<sup>2+</sup>, HgCl<sup>+</sup>, HgCl<sub>2</sub>, HgOHCl, HgOH<sup>+</sup>, and Hg(OH)<sub>2</sub> exist, which could react with thiol group (-SH) as follows [44,45]:



In the strong acidic condition, the dominant species of Hg(II) in the solution were free Hg<sup>2+</sup> ions which could form complexes with mercapto groups (-SH). So the positive charge (-S-Hg<sup>+</sup>) might limit the further entrance of species with positive charge such as Hg<sup>2+</sup> because of electrostatic barriers [46]. Moreover, the formation of positively charged complexes inside the adsorbents could prevent Hg<sup>2+</sup> being replaced with H<sup>+</sup> at a low pH. When the pH of the solution increased, electrostatic barriers were eliminated due to the formation of neutral complexes with (-S-HgOH) in which caused the adsorption capacity to reach a plateau when pH is in the range of 3.0–5.0.

The complexation adsorption of Hg<sup>2+</sup>, Pb<sup>2+</sup> and Ni<sup>2+</sup> on TFNS can be described as follows: [28,46,47]



### E. Adsorption Kinetic

A pseudo-first-order model, Eq. (6), and a pseudo-second-order model, Eq. (7) were used to study the adsorption kinetic model of thiol functionalized nanosilica [28]. The results of the experimental data are shown in Table V.

$$\log\left(1 - \frac{q_t}{q_e}\right) = -\frac{k_1}{2.303} \times t \quad (6)$$

$$\frac{t}{q_t} = \frac{1}{k_2 \times q_e^2} + \frac{1}{q_e} \times t \quad (7)$$

The results illustrated that there was a better correspondence between the pseudo-second-order kinetic model and the adsorption of heavy metals by the adsorbent nanoparticles.

TABLE V  
FITTING DATA OF ADSORPTION KINETIC MODELS OF TFNS FOR Hg, Pb AND Ni IONS

ion	pseudo-first-order			pseudo-second-order		
	$R^2$	$K_1$	$q_e$	$R^2$	$K_2$	$q_e$
Hg	0.925	0.029	13.96	1	0.0073	43.47
Ni	0.969	0.0161	2.80	0.999	0.0395	8.69
Pb	0.971	0.0138	2.89	0.998	0.0392	10.20

### F. Adsorption Isotherm

Equilibrium isotherms studies were carried out in order to determine the optimum conditions for the maximum adsorption of TFNS. The commonly used isotherms for the quantitative description of sorption data are Langmuir isotherm and Freundlich isotherm [48]. The Langmuir isotherm, which is commonly used for the molecular adsorption at interfaces and the prediction of equilibrium parameters [49], was fitted to the adsorption data. The Langmuir model is based on the monolayer adsorption onto homogeneous active sites on adsorbents and can be expressed as Eq. (8).

$$q_e = \frac{q_{\max} K_L C_e}{1 + K_L C_e} \quad (8)$$

where  $q_e$  and  $C_e$  are the adsorption capacity ( $\text{mg g}^{-1}$ ) and the heavy metal concentration at the equilibrium, respectively.  $K_L$  ( $\text{L mg}^{-1}$ ) and  $q_{\max}$  ( $\text{mg g}^{-1}$ ) are respectively the Langmuir constant and the maximum adsorption capacity determined by the intercept and slope of the linear plot of  $C_e/q_e$  versus  $C_e$ .

The Langmuir adsorption isotherm assumes that the adsorbed layer is one molecule in thickness, and that all sites are equal, resulting in equal energies and enthalpies of adsorption [50]. The Langmuir isotherm equation assumes that fixed individual sites exist on the surface of the adsorbent. These sites have equal affinity for the adsorbates in the solution. Each of these sites are capable of adsorbing one molecule, resulting in a layer one molecule thick over the entire adsorbent surface [50]. Unlike the Langmuir isotherm, the Freundlich isotherm, as represented by Eq. (8), does not predict a maximum

sorption amount on the sorbent surface. The Freundlich equation predicts that the concentration of metal ion on the adsorbent will increase as long as there is an increase in the metal ion concentration in liquid, and the adsorbent has heterogeneous adsorption sites with different adsorption potentials and each class of adsorption site adsorbs molecules [51].

$$q_e = K_F C_e^{1/n} \quad (9)$$

$K_F$  is the Freundlich capacity factor,  $C_e$  is the equilibrium concentration of solute in solution after adsorption and  $1/n$  represents Freundlich intensity parameter. The constants in Freundlich isotherm can be determined by plotting  $\log(q_e)$  versus  $\log(C_e)$  and fitting the best straight line to the data.

TABLE VI  
LANGMUIR AND FREUNDLICH ISOTHERM CONSTANTS FOR ADSORPTION OF Hg AND Pb IONS ON TFNS

Langmuir constants			
metal ions	$K_L$ ( $\text{L mg}^{-1}$ )	$q_{\max}$ ( $\text{mg g}^{-1}$ )	$R^2$
Hg	4.01	277.78	0.906
Pb	12.12	67.69	0.945
Freundlich constants			
metal ions	$K_F$ ( $\text{mg g}^{-1}$ ) ( $\text{mg}^{-1}$ ) <sup>1/n</sup>	$1/n$	$R^2$
Hg	166.72	0.801	0.995
Pb	37.24	0.726	0.995

The isotherms, presented in Table VI indicate that adsorption increases with an increase in the equilibrium concentration of the adsorbate. The increase in the initial concentration of Hg(II) provides a greater driving force for the mass transfer between the aqueous solution and the subsequent surface adsorption and integration onto TFNS [52]. As it can be seen from this adsorption, the processes can be correlated with both Langmuir and Freundlich isotherms, but the Freundlich isotherm could fit the sorption data of Hg(II) and Pb(II) on TFNS better than the Langmuir isotherm. According to Giles *et al.* classification [53], the isotherms of Hg(II) and Pb(II) sorption on TFNS were typical H type isotherms, which are the characteristic of chemical adsorption. The isotherms with a marked initial slope indicated that the functionalized materials were acting as high-efficacy adsorbents at low concentrations [28]. The maximum sorption amounts of Hg(II) and Pb(II) on TFNS were 277 and 67  $\text{mg g}^{-1}$ , respectively.

A comparison of the previous studies on heavy metal separation by functional particles is shown in Table VII. These results show that our thiol modified nanosilica is a good adsorbent of Hg ions. As mentioned above, the number of functional groups on the adsorbent surface can determine the adsorption capacity. Therefore, although the prepared TFNS in this study was not porous, due to its high functionalization efficiency, it had high adsorption capacity. This means that the chemical adsorption was the dominate mechanism of Hg adsorption. This high efficiency was achieved because of the functional groups, such as S-H, and the strong affinity of the sulfhydryl groups for mercury and other soft heavy metal.

TABLE VII  
COMPARISON OF PREVIOUS STUDIES OF HEAVY METAL SEPARATION BY FUNCTIONAL PARTICLES

	adsorbent	modifier	ion	initial concentration	adsorption capacity		pH*	ref
					mmol g <sup>-1</sup>	mg g <sup>-1</sup>		
1	SH-functionalized nano-magnetic Fe <sub>3</sub> O <sub>4</sub>	epoxyl-Fe <sub>3</sub> O <sub>4</sub> -co-poly(DVB-MMA-GMA)s + thiourea	Hg (II)	400 mg mL <sup>-1</sup>	1.28	256.7	2 to 6	[44]
2	thiol functional Silica	MPTMS	Pb(II) Cd(II)	250 mg L <sup>-1</sup>	0.62 0.34	130 39	6 5-6	[28]
3	sulfonic acid functional nanoporous Silica	sulfonation of MPTMS modified silica	Pb(II) Cd(II)	1000 mg L <sup>-1</sup>	1.05 1.59	217.9 178.8	5 to 6	[15]
4	thiol functional silica magnetic nanoparticle	MPTMS	Cu(II) Hg(II) Pb(II) Cd(II) Cu(II)	50 mg L <sup>-1</sup>	1.36 0.42 0.34 0.40 0.89	86.6 83.8 70.4 45.2 56.8	4 to 7	[27]
5	mercapto functionalized sepiolite	MPTMS	Pb(II)	180 mg L <sup>-1</sup>	0.47	97	4.2-7	[54]
6	functional silica coated magnetite particles	dithiocarbamate	Hg(II)	50 µg L <sup>-1</sup>	0.12 µmol g <sup>-1</sup>	25 µg g <sup>-1</sup>	-	[20]
7	SH functionalized-MCM-41	MPTMS DETA-TMS	Hg(II)	20 µg L <sup>-1</sup>	1.24	249.3	4 to 6	[14]
8	SH functionalized-MCM-41	2-Mercaptopropyl	Hg(II)	-	0.7	140.2	-	[19]
9	SH functionalized-MCM-41	MPTMS	Hg(II)	-	0.55	110.1	-	[3]
10	SH functional silica aerogel	MPTMS	Hg(II)	20 µg L <sup>-1</sup>	0.9	181	>6	[50]
11	SH functionalized-nanosilica	MPTMS	Hg(II) Pb(II)	40 mg g <sup>-1</sup>	1.38 0.33	277.8 67.69	3-6	This work

\* pH of maximum adsorption

### G. Effect of TFNS on Properties of PES Nocomposite Membrane

In Table VIII, the contact angle of modified and unmodified membranes is presented.

TABLE VIII  
HYDROPHILICITY PROPERTIES OF NANOCOMPOSITE MEMBRANES

samples	contact angle	porosity %
PES	80	80.4
PES-TFS 1	76	74.5
PES-TFS 2	65	72

The static contact angle is declined with adding TFNS to the polymer matrix. In the phase inversion preparation of the nanocomposite membranes, the mixed nanoparticles in the casting solution can migrate spontaneously to the surface of the prepared nanocomposite membranes to reduce the interface energy [55,56]. Although the presence of TFNS decreased the membrane porosity, the influence of nanoparticle concentration on the membrane porosity was not considerable.

Nanocomposite membranes exhibited high adsorption capacity (Table IX). Adsorption capacity of TFNS in nanocomposite membrane was lower than that of free TFNS. In the nanocomposite matrix, the nanoparticles were covered by polymer chains, therefore by increasing the TFNS content, the available free TFNS increased. By increasing the nanoparticle content in the polymeric matrix a strong repulsive force was formed, which led to a strong interfacial stress between the polymer and nanoparticles, and finally interfacial pores due to the shrinkage of organic phase during the demixing process was formed [57]. These defects in membrane formation and the formation of interfacial pores developed the free TFNS particles into membrane pores which led to an increase in the adsorption capacity per unit mass of TFNS.

TABLE IX  
ADSORPTION CAPACITY OF NANOCOMPOSITE MEMBRANES AND TFNS IN THE NANOCOMPOSITE MEMBRANES

Sample	TFNS*	PES-TFS 1	PES-TFS 2
$q_{e,np}$ (mg g <sup>-1</sup> )	277.8	89.76	130.68
$q_{e,m}$ (mg m <sup>-2</sup> )	-	957.9	1326.3

\* Theoretical  $q_{max}$

### IV. CONCLUSION

The thiol-functionalized nanosilica (TFNS) that was prepared in the lowest acidic condition had high grafting efficiency. Adsorption tests on MPTMS modified nanosilica indicated high adsorption capacity for Hg ions. Its adsorption kinetic was consistent with the pseudo-second-order model. The adsorption isotherm of TFNS was consistent with the Freundlich isotherm indicating that MPTMS modified silica nanoparticles had heterogeneous adsorption sites with different adsorption potentials so that each class of adsorption sites adsorbs the molecules. The results demonstrated that isotherms of Hg(II) and Pb(II) sorption on TFNS were typical type isotherms which are the character of the chemical adsorption. The isotherms with a marked initial slope indicated that the functionalized materials acted as high-efficacy adsorbents at low concentrations. The maximum adsorption capacity of the modified nanoparticles showed that TFNS had higher affinity for Hg ions in comparison with Pb and Ni ions, which explicates its selectivity for Hg ions. As mentioned in table VII, the adsorption capacity of prepared TFNS for Hg ions (278 mg g<sup>-1</sup>) was higher than other similar adsorbents. Although prepared TFNS in this study was not porous, whereas, the number of functional groups on the adsorbent surface can determine the adsorption capacity, therefore, the higher functionalization efficiency leads to higher adsorption capacity. This high modification efficiency is a result of the reaction condition. As

observed, the reaction between silica nanoparticles and mercaptosilane was more effective at lower pH. Investigation of membrane adsorption capacity indicated that TFNS could act as a good adsorbent in the PES membrane and significantly increase its separation property. An increase in the TFNS content of PES nanocomposites considerably led to an increase in the membrane adsorption capacity.

#### REFERENCES

- [1] W. Plazinski and W. Rudzinski, "Modeling the effect of surface heterogeneity in equilibrium of heavy metal ion biosorption by using the ion exchange model", *Environ. Sci. Technol.*, vol. 43, pp. 7465–7471, 2009.
- [2] D. Sevdic and H. Meider, "Solvent extraction of silver(I) and mercury(II) by O,ODi-n-butyl R-phenylamino-phenylmethanethio phosphonate from chloride solutions". *Solvent Extr. Ion Exch.*, vol. 8, no. 4-5, pp. 643–658, 1990.
- [3] L. Mercier and T.J. Pinnavaia, "Heavy metal ion adsorbents formed by the grafting of a thiol functionality to mesoporous silica molecular sieves: factors affecting Hg(II) uptake". *Environ. Sci. Technol.*, vol. 32, no. 18, pp. 2749–2754, 1998.
- [4] J. W. Patterson and R. Passino, "Metals Speciation Separation and Recovery", New York: Lewis Publishers, 1990.
- [5] H. Bessbousse, T. Rhlalou, J. F. Verchère, and L. Lebrun, "Sorption and filtration of Hg(II) ions from aqueous solutions with a membrane containing poly(ethyleneimine) as a complexing polymer", *J. Membr. Sci.*, vol. 325, no. 2, pp. 997-1006, 2008.
- [6] A. Rezvani, Boroujeni, M. Javanbakht, M. Karimi, C. Shahrjerdi, and B. Akbari, "Immobilization of thiol-functionalized nanosilica on the surface of poly(ether sulfone) membranes for heavy metal ions removal from industrial wastewater samples". *Ind. Chem. Eng. Res.*, vol. 54, no. 1, pp. 502–513, 2015.
- [7] J. D., Merrifield, W. G. Davids, J. D MacRae, and A. Amirbahman, "Uptake of mercury by thiol-grafted chitosan gel beads", *Water Res.*, vol. 38, no. 13, pp. 3132-3138, 2004.
- [8] T. Budinova, N. Petrov, J. Parra, and V. Baloutzov, "Use of an activated carbon from antibiotic waste for the removal of Hg(II) from aqueous solution", *J. Environ. Manage.* vol. 88, no. 1, pp. 165-172, 2008.
- [9] X. Y. Zhang, Q. C. Wang, S. Q. Zhang, X. J. Sun, and Z. C. Zhang, "Stabilization/solidification (S/S) of mercury-contaminated hazardous wastes using thiol-functionalized zeolite and Portland cement", *J. Hazard. Mater.* vol. 168, no. 2-3, pp. 1575-1580, 2009.
- [10] P. Guo, X. Guo, and C. Zheng, "Roles of  $\gamma$ -Fe<sub>2</sub>O<sub>3</sub> in fly ash for mercury removal: Results of density functional theory study", *Appl. Surf. Sci.*, vol. 256, no. 23, pp. 6991-6996, 2010.
- [11] X. Ma, Y. Li, Z. Ye, L. Yang, L. Zhou, and L. Wang, "Novel chelating resin with cyanoguanidine group: Useful recyclable materials for Hg(II) removal in aqueous environment", *J. Hazard. Mater.*, vol. 185, no. 2-3, pp. 1348-1354, 2011.
- [12] K.S. Xia, R.Z. Ferguson, M. Losier, N. Tchoukanova, R. Brüning, and Y. Djaoued, "Synthesis of hybrid silica materials with tunable pore structures and morphology and their application for heavy metal removal from drinking water", *J. Hazard. Mater.* vol. 183, no. 1-3, pp. 554–564, 2010.
- [13] W. P. Shi, S. Y. Tao, Y. X. Yu, Y. C. Wang, and W. Ma, "High performance adsorbents based on hierarchically porous silica for purifying multicomponent wastewater", *J. Mater. Chem.*, vol. 21, no. 39, pp.15567–15574, 2011.
- [14] S. A. Idris, S. R. Harvey and L. T. Gibson, "Selective extraction of mercury (II) from water samples using mercapto functionalised-MCM-41 and regeneration of the sorbent using microwave", *J. Hazard. Mater.*, vol. 193, no. 1-3, p. 171–176, 2011.
- [15] Q. Qu, Q. Gu, Z. Gu, Y. Shen, C. Wang, and X. Hu, "Efficient removal of heavy metal from aqueous solution by sulfonic acid functionalized nonporous silica microspheres". *Colloid. Surface. A.*, vol. 415, no. 1, pp. 41–46, 2012.
- [16] S. J. Wu, F. T. Li, R. Xu, S. H. Wei, and G. T. Li, "Synthesis of thiol-functionalized MCM-41 mesoporous silicas and its application in Cu(II), Pb(II) Ag(I), and Cr(III) removal", *J. Nanopart. Res.*, vol. 12, no. 6, pp. 2111–2124, 2010.
- [17] G. L. Li, Z. S. Zhao, J. Y. Liu and G. B. Jiang, "Effective heavy metal removal from aqueous systems by thiol functionalized magnetic mesoporous silica", *J. Hazard. Mater.*, vol. 192, no. 1, pp. 277–283, 2011.
- [18] L. C. Lin, M. Thirumavalavan, Y. T. Wang, and J. F. Lee, "Surface area and pore size tailoring of mesoporous silica materials by different hydrothermal treatments and adsorption of heavy metal ions", *Colloid. Surface. A.*, vol. 369, no. 1-3, pp. 223–231, 2010.
- [19] D. P. Quintanilla, A. Sánchez, I. Hierro, M. Fajardo, and I. Sierra, "Preparation, characterization, and Zn<sup>2+</sup> adsorption behavior of chemically modified MCM-41 with 5-mercapto-1-methyltetrazole", *J. Colloid. Interf. Sci.*, vol. 313, no. 2, pp. 551–562, 2007.
- [20] P. I. Girginova, A. L. Dasilva, C. B. Lopes, P. Figueira, M. Otero, V. S. Amaral, E. Pereira, and T. Trindade, "Silica coated magnetite particles for magnetic removal of Hg<sup>2+</sup> from water", *J. Colloid. Interf. Sci.*, vol. 345, no 2, pp. 234-240, 2010.
- [21] M. Javanbakht, M. R. Ganjali, P. Norouzi, A. Badiie, A. Hasheminasab, and M. Abdouss, "Carbon Paste Electrode Modified with Functionalised Nanoporous Silica Gel as a New Sensor for Determination of Silver Ion", *Electroanal.*, vol. 19, no. 12, pp. 1307-1314, 2007.
- [22] M. Javanbakht, F. Divsar, A. Badiie, F. Fatollahi, Y. Khanianid, M. R. Ganjalie, P. Norouzi, M. H. Chalooosi, and Gh. Mohammadi Ziarani, "Determination of picomolar silver concentrations by differential pulse anodic stripping voltammetry at a carbon paste electrode modified with phenylthiourea-functionalised high ordered nanoporous silica gel". *Electrochimica Acta.*, vol. 54, pp. 5381–5386, 2009.
- [23] M. Javanbakht, H. Rudbaraki, M. R. Sohrabi, A. M. Attaran and A. Badiie, "Separation, pre-concentration and determination of trace amounts of lead(II) ions in environmental samples using two functionalised nanoporous silica gels containing a dipyriddy sub-unit". *Intern. J. Environ. Anal. Chem.*, vol. 90, no. 14. pp. 1014–1024, 2010.
- [24] M. Javanbakht A. Badiie, M. R. Ganjali, P. Norouzi, A. Hasheminasab and M. Abdouss, "Use of organofunctionalised nanoporous silica gel to improve the lifetime of carbon paste electrode for determination of copper(II) ions", *Anal. Chim. Acta.* vol. 601, no. 2, pp. 172-182, 2007.
- [25] M. Javanbakht, H. Khoshsafar, M. R. Ganjali, A. Badiie, P. Norouzi and A. Hasheminasab, "Determination of nanomolar mercury(II) concentration by anodic-stripping voltammetry at a carbon paste electrode modified with functionalized nanoporous silica gel", *Curr. Anal. Chem.*, vol. 5, no. 1, pp. 35-41, 2009.
- [26] M. H. Marchena, M. Granada, A.V. Bordoni, M. Joselevich, H. Troiani, F. J. Williams, and A. Wolosiuk, "Organized thiol functional groups in mesoporous core shell colloids". *J. Solid State Chem.*, vol. 187, pp. 97–102, 2012.
- [27] C. Huang and B. Hu, "Silica coated magnetic nanoparticles modified with  $\gamma$ -mercaptopyltrimethoxysilane for fast and selective solid phase extraction of trace amounts of Cd, Cu, Hg and Pb in environmental and biological samples prior to their determination by ICPMS", *Spectrochim. Acta B.*, vol. 63, no. 3, pp. 437-444, 2008.
- [28] X. Liang, Y. Xu, and G. Sun, "Preparation, characterization of thiol functionalised silica and application for sorption of Pb and Cd", *Colloid. Surface A.* vol. 349, no. 1-3, pp. 61-68, 2009.
- [29] C. Barth, M. C. Gonçalves, A. T. N. Pires, J. Roeder, and B. A. Wolf, "A symmetric polysulfone and polyethersulfone membranes: effects of thermodynamic conditions during formation on their performance", *J. Membr. Sci.*, vol. 169, no. 2, pp. 287–299, 2000.
- [30] J. Kim and B. Vander Bruggen, "The use of nanoparticles in polymeric and ceramic membrane structures: Review of manufacturing procedures and performance improvement for water treatment", *Environ. Pollut.*, vol. 158, no. 6, pp. 2335-2349, 2010.
- [31] Y. Yang, H. Zhang, P. Wang, Q. Zheng, and J. Li, "The influence of nano-sized TiO<sub>2</sub> fillers on the morphologies and properties of PSF UF membrane", *J. Membr. Sci.*, vol. 288, no. 1-2, pp. 231-238, 2007.
- [32] T. H. Bae and T. M. Tak, "Effect of TiO<sub>2</sub> nanoparticles on fouling mitigation of ultrafiltration membranes for activated sludge filtration", *J. Membr. Sci.*, vol. 249, no. 1-2, pp. 1-8, 2005.
- [33] C. S. Zhao, J. Xue, F. Ran, and S. Sun, "Modification of polyethersulfone membranes – A review of methods", *Prog. Mater.*

- Sci.*, vol. 58, no. 1, pp. 76–150, 2013.
- [34] M. I. Mrkoci, "Influence of silica surface characteristics on elastomer reinforcement" M.Sc. thesis, Queen's University Kingston, Ontario, Canada, 2001.
- [35] M. Rostami, M. Mohseni and Z. Ranjbar, "Investigating the effect of pH on the surface chemistry of an amino silane treated nano-silica", *Pigm. Resin Technol.*, vol. 40, no. 6, pp. 363-373, 2011.
- [36] C. H. Lee, S. H. Park, W. Chung, J. Y. Kim and S. H. Kim, "Preparation and characterization of surface modified silica nanoparticles with organo-silane compounds". *Colloid. Surf. A.*, vol. 384, no. 1-3, pp. 318– 322, 2011.
- [37] C. Piao, J. E. Winandy, and T. F. Shupe, "From hydrophilicity to hydrophobicity, a critical review: Part I. Wettability and Surface Behavior", *Wood Fiber Sci.*, vol. 42, no. 4, pp.1–21, 2010.
- [38] R. G. Pearson, "Hard and soft acids and bases", *J. Am. Chem. Soc.*, vol. 85, no. 22, pp. 3533-3539, 1963.
- [39] L. Mercier and L. Detellier, "Preparation, characterization, and applications as heavy metals sorbents of covalently grafted thiol functionalities on the interlamellar surface of montmorillonite", *Environ. Sci. Technol.*, vol. 29, no. 5, pp. 1318–1323, 1995.
- [40] C. F. Baes and R. E. Mesmer, "The hydrolysis of cations", New York: Wiley, 1976.
- [41] A. Arencibia, J. Aguado, and J. M. Arsuaga, "Regeneration of thiol-functionalised mesostructured silica adsorbents of mercury", *Appl. Surf. Sci.* vol. 256, no.17, pp. 5453-5457, 2010.
- [42] E. F. S. Vieira, A. R. Cestari, J. De, A. Simoni, and C. Airoidi, "Use of calorimetric titration to determine thermochemical data for interaction of cations with mercapto modified silica gel", *Thermochim. Acta.*, vol. 328, no. 1-2, pp. 247–252, 1999.
- [43] A. Walcabius, J. Devoy, and J. Bessiere, "Electrochemical recognition of selective mercury adsorption on minerals", *Environ. Sci. Technol.* vol. 33, no. 23, pp. 4278–4284, 1999.
- [44] S. Pan, Y. Zhang, H. Shen, and M. Hu, "An intensive study on the magnetic effect of mercapto-functionalized nano-magnetic Fe<sub>3</sub>O<sub>4</sub> polymers and their adsorption mechanism for the removal of Hg(II) from aqueous solution", *Chem. Eng. J.*, vol. 210, pp. 564–574, 2012.
- [45] J. Wang, B. L. Deng, X. R. Wang and J. Z. Zheng, "Adsorption of aqueous Hg(II) by sulfur-impregnated activated carbon", *Environ. Eng. Sci.*, vol. 26, no. 12, pp. 1693–1699, 2009.
- [46] A. Walcarius and C. Delacote, "Mercury (II) binding to thiol functionalized mesoporous silicas: critical effect of pH and sorbent properties on capacity and selectivity", *Anal. Chim. Acta.*, vol. 547, no. 1, pp. 3–13, 2005.
- [47] D. Bagal-Kestwal, M. S. Karve, B. Kakade, and V. K. Pillai, "Invertase inhibition based electrochemical sensor for the detection of heavy metal ions in aqueous system: application of ultra-microelectrode to enhance sucrose biosensor's sensitivity", *Biosens. Bioelectron.*, vol. 24, pp. 657–664, 2008.
- [48] H. B. Bradl, "Adsorption of heavy metal ions on soils and soils constituents", *J. Colloid Interface Sci.* vol. 277, no. 1, pp. 1–18, 2004.
- [49] Y. S. Ho, "Selection of optimum sorption isotherm", *Carbon*, vol. 42, no.10, pp. 2115–2116, 2004.
- [50] U. Štandeker, A. Veronovski, Z. Novak, and Z. Knez, "Silica aerogels modified with mercapto functional groups used for Cu(II) and Hg(II) removal from aqueous solutions. *Desalination*, vol. 269, no. 1-2, pp. 223–230, 2011.
- [51] M. A. Al-Ghouti, M. A. M. Khraisheh, M. N. M. Ahmad and S. Allen, "Adsorption behavior of methylene blue onto Jordanian diatomite: A kinetic study", *J. Hazard. Mater.*, vol. 165, no.1-3, pp. 589-598, 2009.
- [52] C. Giles, T. Mac Ewan, S. Nakhwa, and D. Smith, "Studies in adsorption. Part XI. A system of classification of solution adsorption isotherms, and its use in diagnosis of adsorption mechanisms and in measurement of specific surface areas of solids", *J. Chem. Soc.*, vol. 3, no. 1, pp. 3973–3993, 1960.
- [53] A. A. P. Mansur, O. L. D. Nascimento, W. L. Vasconcelos and H. S. Mansur, "Chemical Functionalisation of Ceramic Tile Surfaces by Silane Coupling Agents: Polymer Modified Mortar Adhesion Mechanism Implications", *J. Mater. Res.*, vol. 11, no. 3, pp. 293-302, 2008.
- [54] X. Liang, Y. Xu, L. Wang, Y. Sun, D. Lin, X. Qin, and Q. Wan, "Sorption of Pb<sup>2+</sup> on mercapto functionalized sepiolite", *Chemosphere*, vol. 90, no. 2, pp. 548-55, 2013.
- [55] V. Vatanpour, S. S. Madaeni, R. Moradian, S. Zinadini, and B. Astinchap, "Fabrication and characterization of novel antifouling nanofiltration membrane prepared from oxidized multi walled carbon nanotube/polyethersulfone nanocomposite", *J. Membr. Sci.*, vol. 375, no. 1-2, pp. 284–294, 2011.
- [56] M. Sun, Y. Su, C. Mu, and Z. Jiang, "Improved antifouling property of PES ultrafiltration membranes using additive of silica-PVP nanocomposite", *Ind. Eng. Chem. Res.*, vol. 49, no. 2, pp. 790–796, 2010.
- [57] K. De Sitter, C. Dotremont, I. Genné, and L. Stoops, "The use of nanoparticles as alternative pore former for the production of more sustainable polyethersulfone ultrafiltration membranes", *J. Membr. Sci.*, vol. 471, no. 1-2, pp. 168-176, 2014.